

Article

Pd on the Composite of Perlite and Allylamine-*N*-isopropylacrylamide Copolymer: A Thermo-Responsive Catalyst for Hydrogenation of Nitroarenes under Mild Reaction Condition

Neda Abedian-Dehaghani ¹, Majid M. Heravi ^{1,*} and Samahe Sadjadi ^{2,*} 

¹ Department of Chemistry, School of Physics and Chemistry, Alzahra University, Vanak, Tehran 1993891176, Iran; n.abedian@alzahra.ac.ir

² Gas Conversion Department, Faculty of Petrochemicals, Iran Polymer and Petrochemical Institute, Tehran 14975112, Iran

* Correspondence: mmh1331@yahoo.com or mmheravi@alzahra.ac.ir (M.M.H.); s.sadjadi@ippi.ac.ir (S.S.)



Citation: Abedian-Dehaghani, N.; Heravi, M.M.; Sadjadi, S. Pd on the Composite of Perlite and Allylamine-*N*-isopropylacrylamide Copolymer: A Thermo-Responsive Catalyst for Hydrogenation of Nitroarenes under Mild Reaction Condition. *Catalysts* **2021**, *11*, 1334. <https://doi.org/10.3390/catal11111334>

Academic Editors: Salam Titinchi and Hanna Abbo

Received: 4 October 2021

Accepted: 1 November 2021

Published: 4 November 2021

Publisher's Note: MDPI stays neutral with regard to jurisdictional claims in published maps and institutional affiliations.



Copyright: © 2021 by the authors. Licensee MDPI, Basel, Switzerland. This article is an open access article distributed under the terms and conditions of the Creative Commons Attribution (CC BY) license (<https://creativecommons.org/licenses/by/4.0/>).

Abstract: A novel thermo-responsive catalyst for the hydrogenation of nitroarenes under mild reaction condition was devised. To prepare the catalyst, a thermo-responsive polymer was first synthesized through the co-polymerization of *N*-isopropylacrylamide and allylamine and then covalently grafted on the Cl-functionalized perlite. The resulting composite was subsequently utilized as a support for the stabilization of Pd nanoparticles. Investigation of the catalytic activity of the catalyst approved its high catalytic activity at a temperature above the lower critical solution temperature. More precisely, 0.03 g of the catalyst can promote the reaction of 1 mmol of nitro-compounds in H₂O/EtOH (1:1) at 45 °C to furnish the corresponding products in 70–100% yields. This issue was assigned to the collapse of the polymeric component and formation of a hydrophobic environment that was beneficial for the mass-transfer of the hydrophobic nitroarenes. Notably, the catalytic activity of the catalyst was higher than that of palladated perlite and thermos-responsive polymer due to the synergistic effects between the perlite and polymeric moiety. Furthermore, the study of the substrate scope confirmed that a wide range of substrates with different steric and electronic properties could tolerate hydrogenation reaction. Moreover, the catalyst was highly selective toward hydrogenation of the nitro group and could be recycled up to seven runs with insignificant Pd leaching and loss of catalytic activity. The hot filtration test also confirmed the heterogeneous nature of the catalysis.

Keywords: heterogeneous catalyst; perlite; thermo-responsive polymer; hydrogenation

1. Introduction

Devising cost-effective heterogeneous catalysts is an important subject in the field of catalysis. In this context, use of natural compounds for the immobilization of catalytic species has attracted particular attention. Perlite (Per) is an amorphous volcanic glass that is generated through rapid cooling of a viscous lava [1–8]. This low-cost volcanic rock, which contains ~70–75% of SiO₂ and 12–18% of Al₂O₃ is highly stable, none-corrosive, non-toxic, and easy to handle [1,2,9–12]. Thanks to the presence of siloxane groups, Per can be chemically modified by organic moieties. To date, various catalysts based on functionalized Per have been reported [1]. As an example, TiO₂ nanoparticles have been stabilized on Per granules and successfully used for the photocatalytic degradation of ammonia in wastewater [13]. Moreover, synthesis of Pd/Per nanocomposite and its catalytic activity have been reported [14].

Stimuli-responsive polymers, mostly referred to as smart polymers, are polymers that respond to different stimuli such as pH [15], temperature [16,17], light [18], electro-field, and oxidizing/reducing agents, etc. [19–21]. In recent years, this class of polymer has

attracted considerable attention due to their applications in various domains such as matrix chemistry, thermochromic and electrochromic materials, biomedical fields, etc. [22,23].

One of the most widely utilized thermo-responsive polymers is poly(*N*-isopropylacrylamide) (PNIPAM). This polymer displays thermo-responsive behavior that produces a phase-separation (i.e., coil-to-globule transition) in the aqueous solution at a lower critical solution temperature (LCST) [24]. Such a dehydration and phase separation is caused by altering the hydrogen bonds between the PNIPAM network and H₂O molecules below and above LCST [24,25]. More recently, copolymers of PNIPAM have been extensively studied. As an example, allylamine-*N*-isopropylacrylamide copolymer with LCST about 34 °C have been used to design smart catalysts [26].

Among the various types of hydrogenation reactions [27,28], hydrogenation of nitro-compounds is of great importance [29–31]. This class of hydrogenation reaction not only can be applied for the synthesis of fine chemicals, but is also applicable for environmental remediation. Similar to other hydrogenation reactions, reduction in nitro-compounds proceeds with the aid of a hydrogen source and a catalytic species [32,33]. The conventional catalyst for this process is supported Pd species. Among various supporting materials, natural compounds that benefit from low-cost, availability, low-toxicity, and biocompatibility are of priority. To date, various natural compounds such as clays [34] and carbohydrates [35] have been utilized for the immobilization of Pd nanoparticles.

In the continuation of our research on using natural compounds for the design of heterogeneous catalysts [36,37], in this article, we wish to report the synthesis of a thermo-responsive catalyst, Pd@Per-P. To prepare the catalyst, Per was covalently functionalized with a thermo-responsive polymer and then utilized as a support for the immobilization of Pd nanoparticles (Figure 1). The activity and recyclability of the catalyst were appraised for the hydrogenation of nitroarenes under a mild reaction condition.

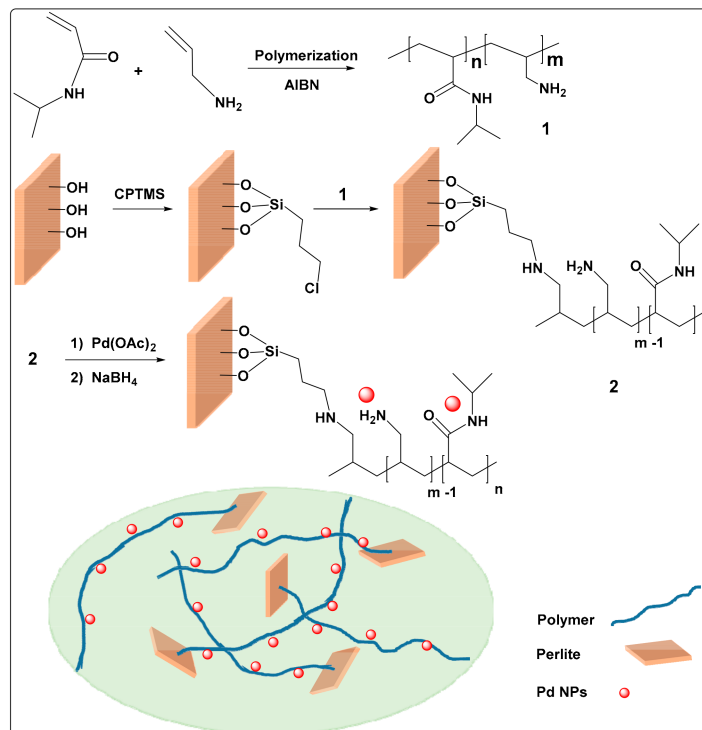


Figure 1. Synthetic method for the preparation of Pd@Per-P.

2. Results and Discussion

2.1. Catalyst Characterization

The SEM image of Per and the as-prepared catalyst are depicted in Figure 2. As illustrated, Per possesses a sheet-like morphology. In the case of the SEM image of the

catalyst, Per sheets can also be detected. On the other hand, tiny aggregates that can be assigned to the polymeric component can be observed on the Per sheets.

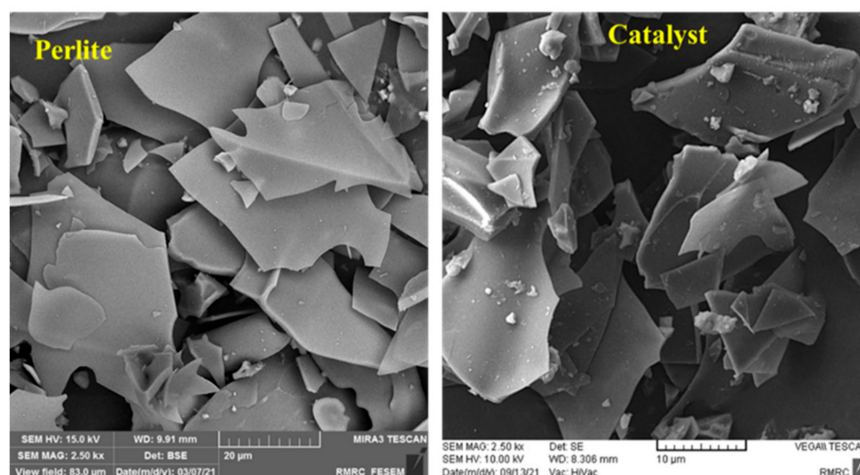


Figure 2. SEM images of Per and the as-prepared catalyst.

EDS and elemental mapping analyses of Pd@Per-P are presented in Figures 3 and 4. According to the EDS analysis, the catalyst contains Ca, Si, Al, O, Fe, K, Na, C, N, and Pd atoms. Among the aforementioned atoms, Ca, Si, Al, O, Fe, K, and Na can be ascribed to the Per structure, while C, N, and O atoms are indicative of the polymeric component in the structure of the catalyst. Moreover, high dispersion of C and N atoms in the elemental mapping analysis could indicate that the polymeric component was uniformly formed on Per. Similarly, it can be concluded that Pd nanoparticles have been homogeneously immobilized on Per-P.

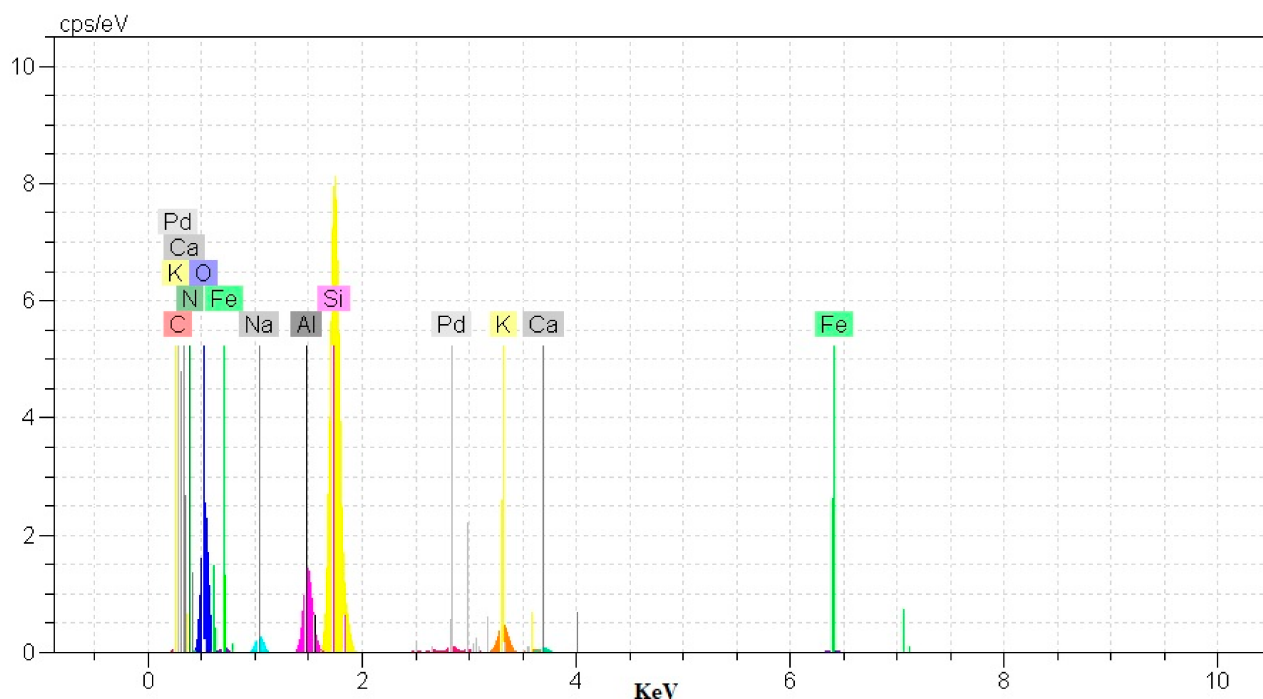


Figure 3. EDS analysis of the as-prepared catalyst.

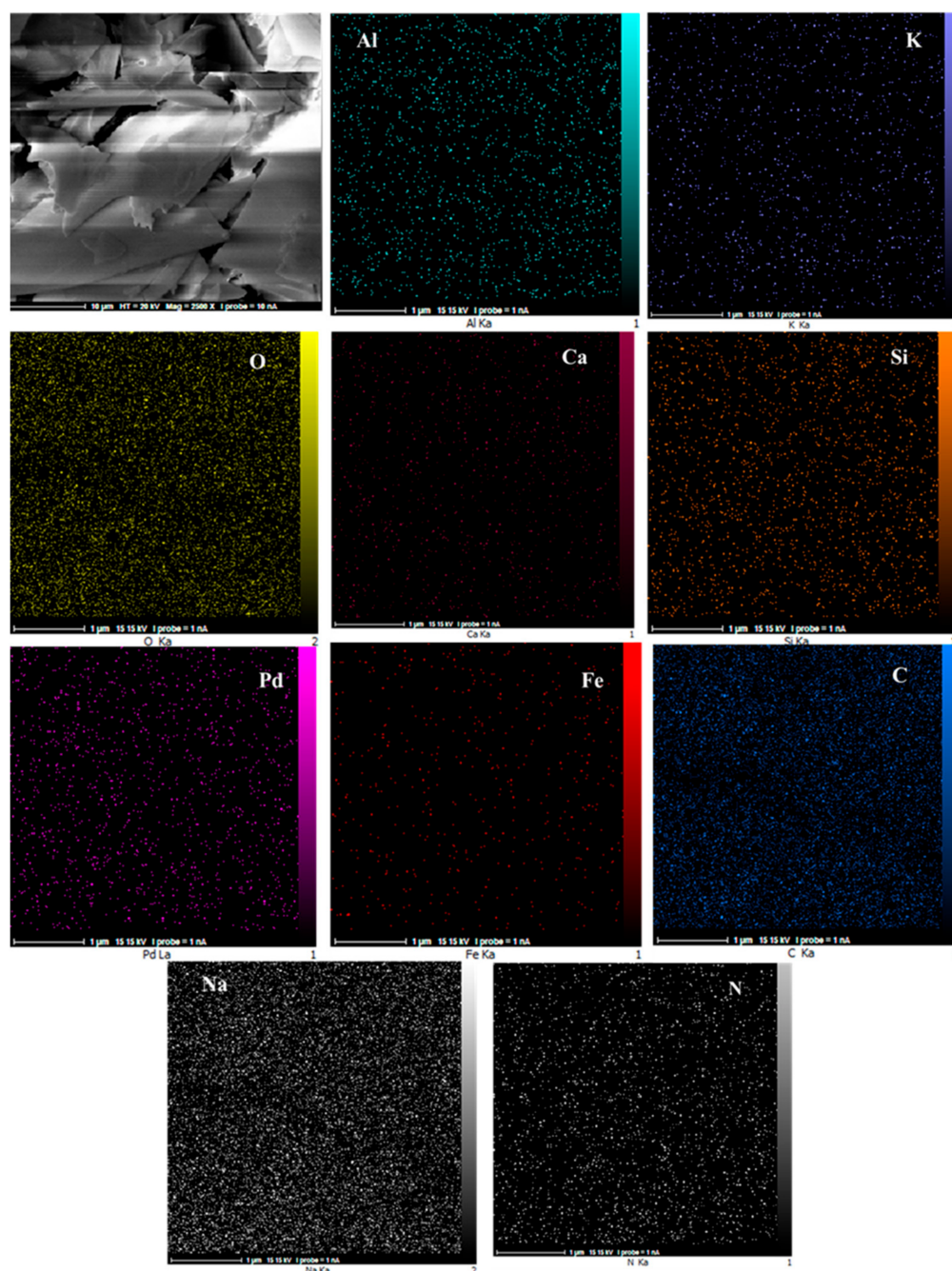


Figure 4. Elemental mapping analysis of Pd@Per-P.

The TEM image of the catalyst is shown in Figure 5. In this image, apart from Per (dark area), the polymeric sheet can also be detected. Moreover, it can be observed that Pd nanoparticles (with average diameter of 4 ± 0.2 nm) were dispersed on the composite homogeneously.

XRD analysis was used to examine the crystal phases of Per and Pd@Per-P (Figure 6). As shown, Per has an amorphous mineral phase and showed a broad band in the range of $2\theta = 10\text{--}34^\circ$ [38]. In the XRD pattern of Pd@Per-P, the characteristic band of Per (i.e., the broad band at $2\theta = 10\text{--}34^\circ$) as well as small bands at $2\theta = 40.3^\circ$ and 45.7° could be detected. These peaks can be assigned to Pd nanoparticles. Notably, other characteristic bands of Pd nanoparticles are not detectable due to their low intensities.

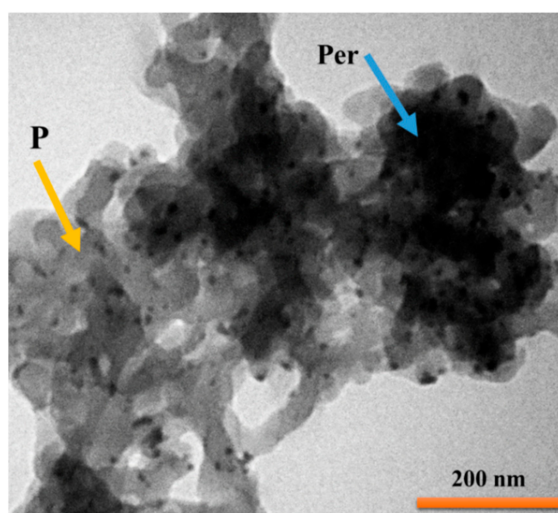


Figure 5. TEM image of the catalyst.

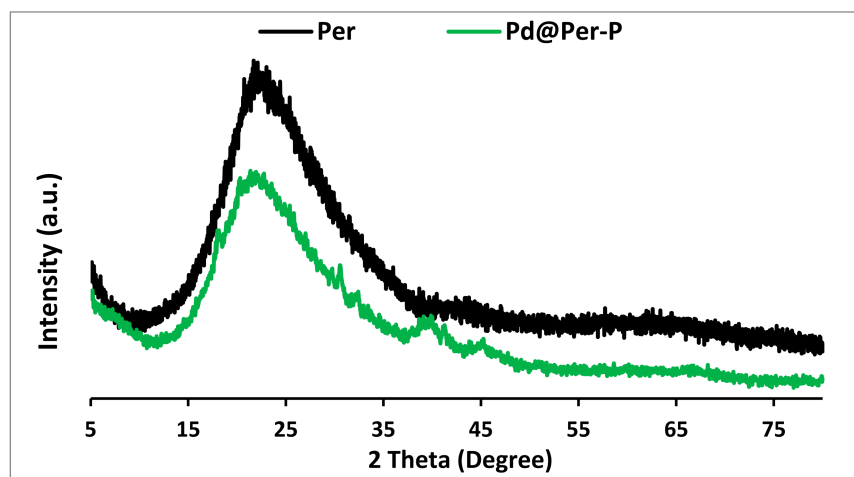


Figure 6. Comparison of the XRD patterns of Per and Pd@Per-P.

FTIR spectra of Per, Per-Cl, P, and Pd@Per-P are depicted in Figure 7. In the spectrum of Per, the absorbance band at 3407 cm^{-1} is related to the -OH group [39], while the band at 460 cm^{-1} is due to the rocking motion of the bridging oxygen atom perpendicular to the Si-O-Si plane. Furthermore, the band at 1059 cm^{-1} can be ascribed to the stretching vibration of Si-O-Si or Si-O-Al . The absorption band at 792 cm^{-1} is due to the Si-O stretching vibration of Si-O-Al [12]. Comparison of the FTIR spectrum of Per and Per-Cl indicated that the FTIR spectrum of Per-Cl showed two additional bands at 2926 cm^{-1} and 582 cm^{-1} , which are illustrative of -CH_2 and -C-Cl stretching vibration, respectively, confirming conjugation of CPTMC [40]. In the FTIR spectrum of P, the bands located at 1654 cm^{-1} and 1545 cm^{-1} were assigned to the amide group, while those at 1461 cm^{-1} , 1386 cm^{-1} , and 1367 cm^{-1} were assigned to the stretching vibrations of the isopropyl group [26]. Moreover, the bands located at $2876\text{--}2973\text{ cm}^{-1}$ were illustrative of stretching vibrations of aliphatic -C-H . The bands located at 3069 cm^{-1} and 3283 cm^{-1} were assigned to -N-H of amine and amide groups. In the Pd@Per-P spectrum, the characteristic bands of Per and thermo-responsive P could be seen, which is an indication of the catalyst formation.

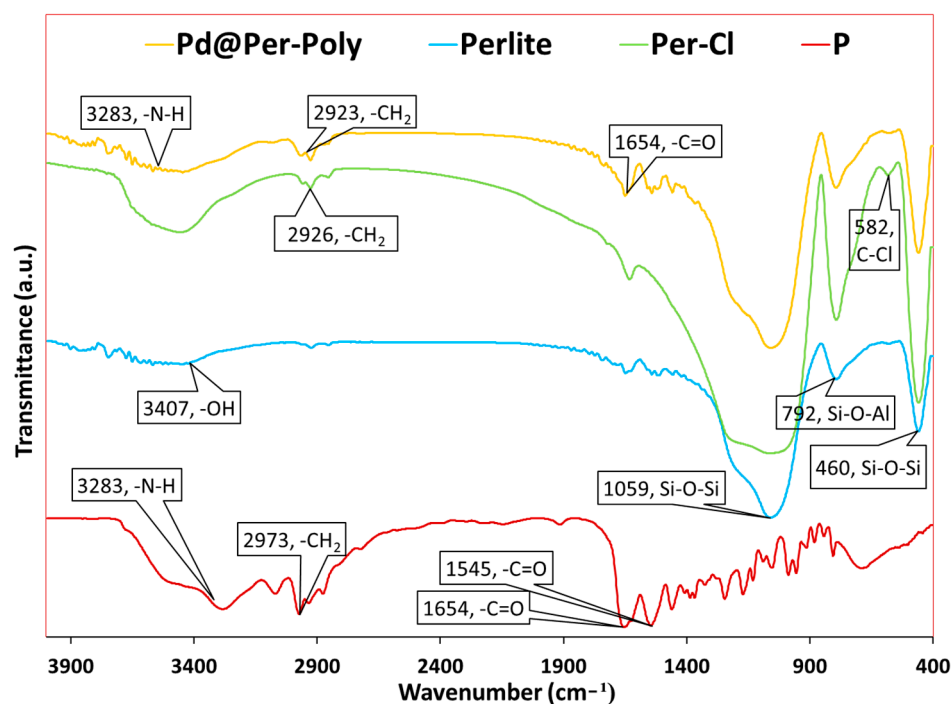


Figure 7. FTIR spectra of Per, Per-Cl, P, and Pd@Per-P.

Thermal stability of Pd@Per-P was studied by TGA. The thermograms of Per and Pd@Per-P are illustrated in Figure 8. The results showed that Per had a weight loss below 120 °C, which is due to the evaporation of physically adsorbed water. Moreover, a steady weight loss at 570 °C can be attributed to the dihydroxylation of Per [1]. Pd@Per-P displayed three weight loss steps. The first weight loss was related to the loss of water, the weight loss in the range of 300–400 °C (20 wt.%) could be due to the decomposition of polymeric component (P) [41,42] and the third weight loss was due to the dihydroxylation of Per.

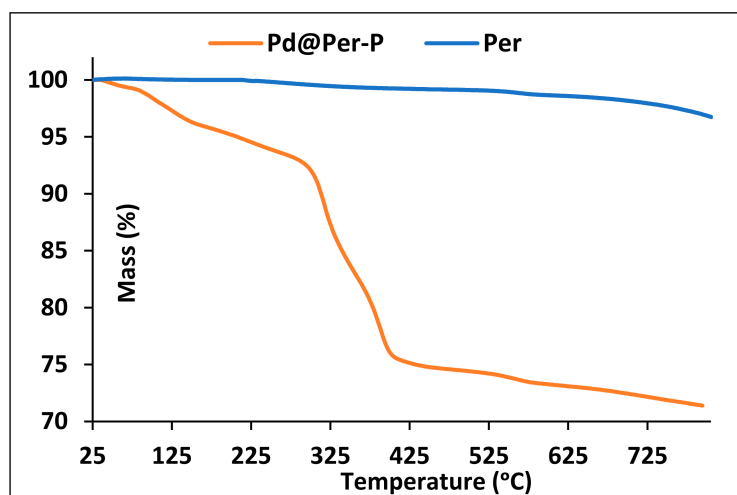


Figure 8. TG curves of Per and Pd@Per-P.

The textural properties of Pd@Per-P have also been studied via BET. The results showed that the specific surface area of the catalyst was 2.41 m²·g^{−1}. Additionally, the N₂ adsorption–desorption isotherm of the catalyst, illustrated in Figure 9, was of type II, implying that Pd@Per-P contains a macroporous or non-porous nature.

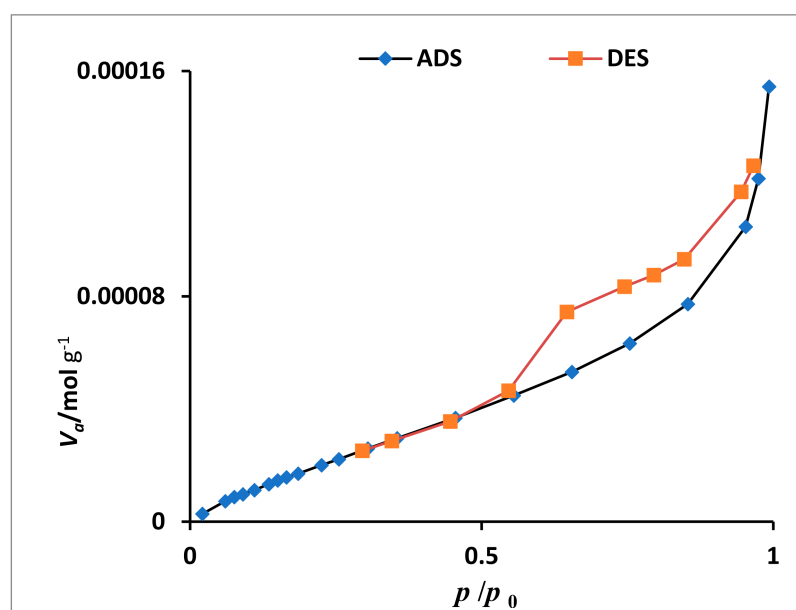


Figure 9. N₂ adsorption–desorption isotherm of Pd@Per-P.

2.2. Activity

The catalytic activity of Pd@Per-P as a thermo-responsive catalyst was assessed for the hydrogenation of nitro-aromatic compounds (Figure 10b). Initially, synthesis of aniline from hydrogenation of nitrobenzene was selected as a model reaction. To achieve an environmentally benign procedure, water was selected as the solvent and hydrogen gas (1 atm) was used as the reducing agent. According to the literature [24,26], it was expected that at a temperature above the LCST (34 °C), the polymeric component on the structure of the catalyst collapses to generate a hydrophobic environment that is beneficial for the mass-transfer of hydrophobic substrates (Figure 10a). To verify this issue, the model reaction was carried out in the presence of 30 mg of Pd@Per-P at three different temperatures (25, 45 and 50 °C). The results (Table 1) indicated that at a temperature below LCST (25 °C), the yield of the reaction was lower than the temperature above LCST. According to these results, 45 °C was selected as the best reaction temperature. To further improve the yield of the model reaction, the effect of the reaction solvent was investigated. The results in Table 1 indicate that the mixture of H₂O:EtOH (1:1) was more efficient than water and the other examined solvents and performing the reaction in the presence of 30 mg of Pd@Per-P in H₂O:EtOH (1:1) at 45 °C led to the formation of aniline in 98% yield. Finally, to appraise the effect of the loading of Pd@Per-P, the model reaction was repeated under the aforementioned condition in the presence of various amounts of the catalyst. The results implied that 30 mg was the optimum amount of the catalyst and use of a lower content of the catalyst resulted in a lower yield of the model product.

Table 1. Optimization of the experimental conditions for the hydrogenation of nitroarenes.

Entry	Pd@Per-P (mg)	Solvent	Temp. (°C)	Yield (%) ^a
1	20	H ₂ O	25	60
2	20	EtOH	25	68
3	20	CH ₃ CN	25	64
4	20	THF	25	56
5	20	H ₂ O:EtOH (1:1)	25	70
6	20	H ₂ O:EtOH (1:1)	45	85
7	20	H ₂ O:EtOH (1:1)	50	85
8	30	H ₂ O:EtOH (1:1)	45	98

^a Reaction condition: nitrobenzene (1 mmol), H₂O:EtOH (1:1) (10 mL), hydrogen flow: 50 mL/min, agitation (700 rpm).

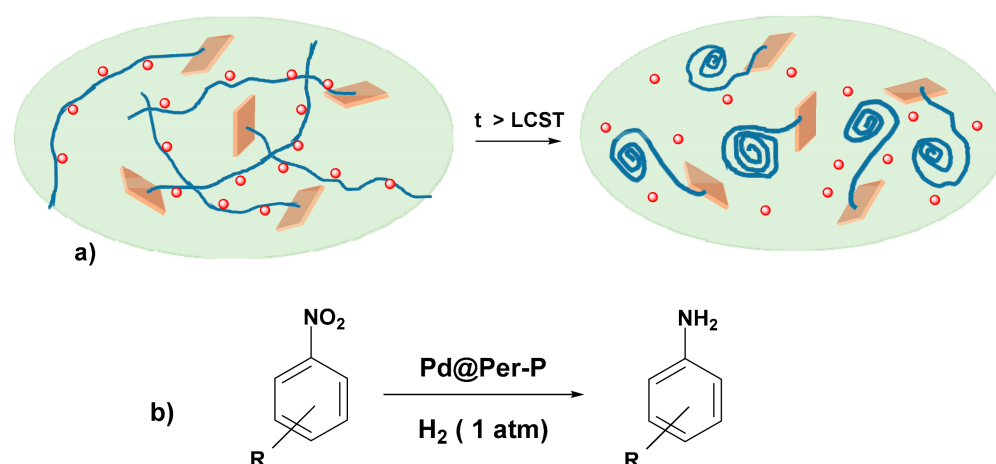


Figure 10. (a) Schematic representation of the structural change of Pd@Per-P at temperature above LCST. (b) Hydrogenation of nitroarenes.

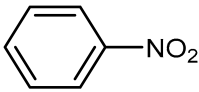
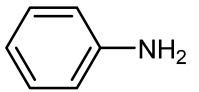
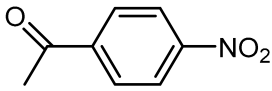

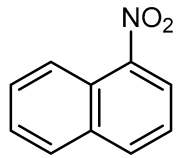
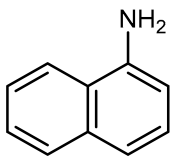
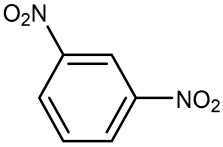
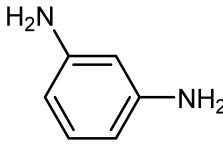
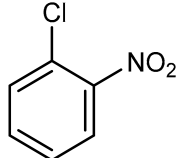
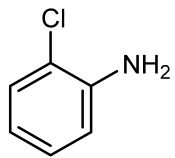
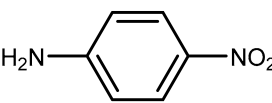
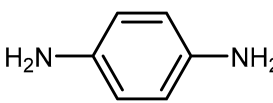
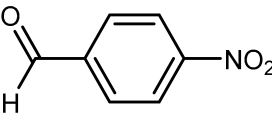
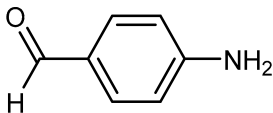


2.3. Comparison with Control Catalysts

One of the most important issues in catalysis is the simplicity of the catalysts. Therefore, the catalysts that can be prepared easily through facile synthetic procedures and cost-effective raw materials are of great interest. On the other hand, the catalytic performance is a crucial factor. In this study, it was assumed that hybridization of Per, which is a low-cost support with a thermo-responsive polymer, could enhance the activity of the resultant catalyst. To validate this assumption and to appraise whether the presence of the thermo-responsive polymer was necessary for achieving high catalytic activity, a control catalyst, Pd@Per, was prepared through palladation of Per via the same procedure used for the palladation of Per-P and its catalytic activity for the model hydrogenation reaction under the optimized condition was examined. Interestingly, it was found that this control catalyst exhibited low catalytic activity (20%). On the other hand, a second control catalyst, Pd@P, was prepared through a similar procedure used for the synthesis of the catalyst, except that P was applied as a support instead of Per-P. Studying the activity of this control catalyst showed that this catalyst led to the formation of aniline in 56%. These results indicate that immobilization of Pd nanoparticles on the composite of P and Per significantly improved the activity of the resulting catalyst. This may be due to the synergistic effect between P and Per.

2.4. Substrate Scope

To confirm the generality of this methodology, hydrogenation of various nitroarenes was carried out under the optimum reaction condition. As listed in Table 2, nitroarenes with electron-donating and electron-withdrawing groups can undergo hydrogenation reaction to furnish the corresponding products in high yields. Furthermore, hydrogenation of 1-nitro naphthalene, which is a sterically demanding substrate, proceeded efficiently to give the desired product in excellent yield. Notably, the required reaction time for this nitro-compound was longer than the other examined nitroarenes. In the case of 1,3-dinitrobenzene, which contains two nitro-functionalities, both nitro groups were hydrogenized to furnish 1,3-diaminobenzene in high yield.

Table 2. Hydrogenation of various nitroarenes under Pd@Per-P catalysis.

Entry	Substrate	Product	Time (min)	Yield (%)
1			90	98
2			120	95
3			150	98
4			120	95
5			150	70
6			150	95
7			110	100
8			135	90

Reaction condition: nitroarenes (1 mmol), catalyst (0.03 g), solvent (H₂O/EtOH; 1:1 (10 mL), temperature 45 °C, H₂ (1 atm).

2.5. Selectivity of Pd@Per-P

To investigate the selectivity of Pd@Per-P toward the hydrogenation of nitro groups, two substrates (i.e., 4-nitroacetophenone and 4-nitrobenzaldehyde) that contain competing functionalities were hydrogenized under Pd@Per-P catalysis. The results (Table 2) imply that both of the aforementioned substrates were selectively hydrogenated to furnish 4-aminoacetophenone and 4-aminobenzaldehyde as sole products in high yields. This experiment approved high selectivity of Pd@Per-P toward the hydrogenation of the nitro group.

2.6. Comparative Study

Although the main target of this research was the development of a thermo-responsive catalyst based on Per and poly(NIPAM-co-AAm) and the hydrogenation of nitroarenes was selected only as a model chemical transformation to examine the catalyst performance, a comparative study was conducted to appraise whether the activity of Pd@Per-P was comparable with other reported catalytic systems. To this purpose, the activity of the catalyst for the model reaction was compared with some other catalysts that have been reported for this reaction by using hydrogen gas as a reducing agent and Pd-based catalysts. In Table 3, the comparison of the reaction time, temperature, solvent, hydrogen pressure, and yield

of the model product for each catalytic system has been reported. As shown, some of the reported methodologies utilized high hydrogen pressure that is neither safe nor economic. In one procedure, a hazardous solvent was applied that is not environmentally benign. Comparing the reaction conditions and yields of other protocols, it can be concluded that Pd@Per-P exhibited high activity, which is comparable or even higher than some of the previously reported catalysts.

Table 3. The comparison of the activity of Pd@Per-P for the model hydrogenation reaction.

Entry	Catalyst	Solvent	Time (min)	Temp. (°C)	H ₂ Pressure	Yield (%)	Ref.
1	Pd@Per-P (0.03 g)	H ₂ O: EtOH (1:1)	90	45	1 atm	98	This work
2	Pd@Hal-Hydrogel+cyclodextrin (2 wt.%)	H ₂ O	120	50	1 bar	95	[43]
3	PdNP (0.5%)/Al ₂ O ₃ (0.3 g)	THF	180	r.t.	1 atm	100	[44]
4	Pd@Hal-TCT-Met ^a	H ₂ O	75	65	1 bar	100	[45]
5	APSNP ^b (1 mol%)	EtOH	120	r.t.	40 atm	100	[46]
6	Pd@CS-CD-MGQDs ^c (0.5 mol%)	H ₂ O	60	50	1 atm	97	[47]
7	Pd/PPh ₃ @FDU-12 (8.33 × 10 ^{−4} mmol Pd)	EtOH	60	40	10 bar	99	[48]
8	Pd@Hal-biochar ^d (0.03 mol%)	H ₂ O	60	r.t.	1 bar	75	[49]
9	Pd@Hal/di-urea ^e (1.5 wt%)	H ₂ O	60	50	1 atm	100	[32]
10	Pd@Hal-CCD ^f (1 wt%)	H ₂ O	90	r.t.	1 atm	100	[50]

^a Pd immobilization on the multi-amine functionalized halloysite. ^b Activated palladium sucrose nanoparticles. ^c Pd on hybrid of magnetic graphene dots and cyclodextrin decorated chitosan. ^d Hybrid of halloysite and char. ^e Halloysite clay decorated with ligand. ^f Halloysite decorated with cyclodextrin derived carbon sphere.

2.7. Recyclability

To evaluate the recyclability of Pd@Per-P, the recycled catalyst from hydrogenation of nitroarene was washed with toluene, dried, and applied for the next run of the same reaction under similar conditions. Recovery and recycling were repeated for seven consecutive runs and the yield of aniline for each run was obtained (Figure 11). Comparison of the obtained yields confirmed that the activity of Pd@Per-P decreased slightly upon each recycling run.

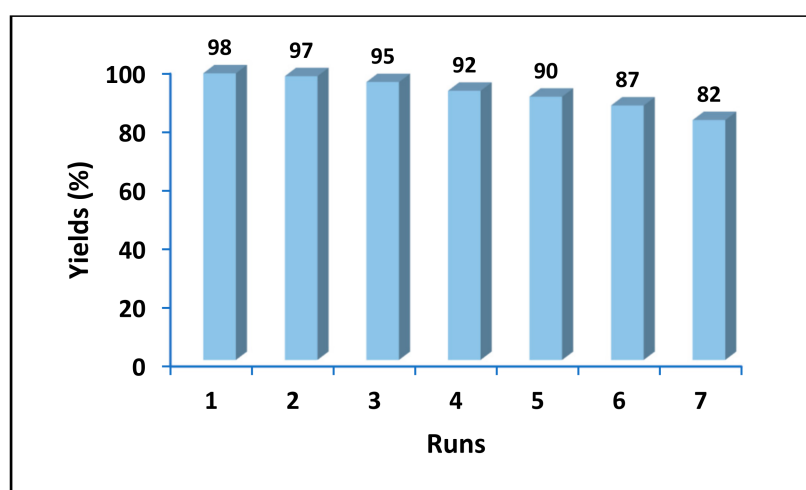


Figure 11. The yields of the model product for seven reaction runs by using the recovered Pd@Per-P under optimum reaction condition.

To investigate the origin of the loss of the activity of Pd@Per-P upon recycling, the FTIR spectrum of the recycled catalyst (after seven runs) was compared with that of the fresh catalyst. As shown in Figure 12, the FTIR spectra of the reused and fresh Pd@Per-P

were very similar. In fact, all of the absorbance bands of fresh Pd@Per-P were detectable in the FTIR spectrum of the reused catalyst, indicating the stability of Pd@Per-P upon recycling.

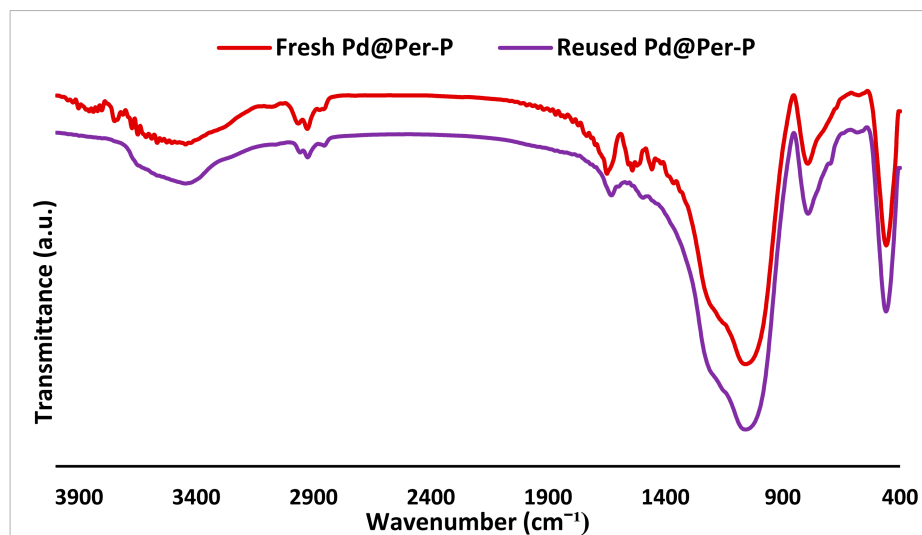


Figure 12. FTIR spectra of fresh and recycled Pd@Per-P after seven runs of the model reaction under optimum conditions.

Next, to elucidate whether recycling can induce Pd leaching, the recycled Pd@Per-P after the seventh run was analyzed via ICP analysis. Comparison of the Pd content of the fresh and recycled Pd@Per-P (recovered from the seventh run) implied that recycling can result in slight Pd leaching (1.2 wt.% of the initial loading). This issue can justify the decrement of the activity of the catalyst.

In fact, visual comparison of the color of the fresh and reused Pd@Per-P (Figure 13) affirmed that even after seven reaction runs, the catalyst preserved its grayish color. This issue can indicate that the Pd leaching was low.

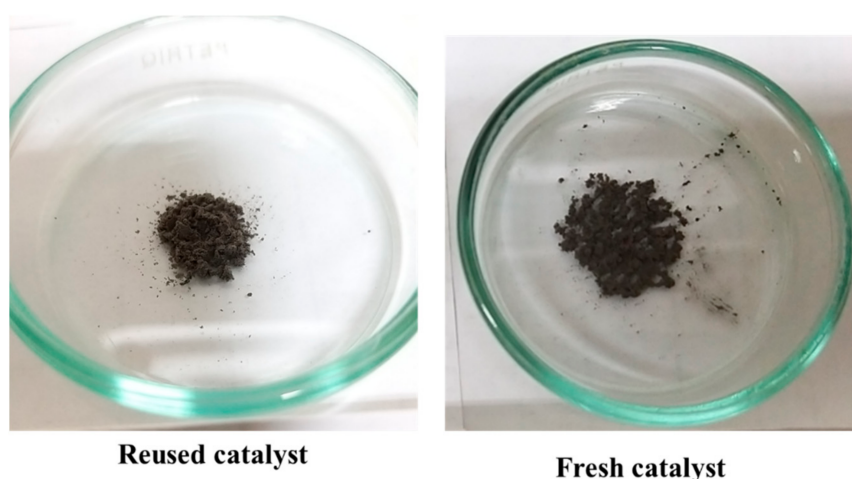


Figure 13. Comparison of the color of the fresh and reused catalyst.

To study the effect of recycling on the catalyst morphology, TEM images of the recycled catalyst (after seventh run) were obtained (Figure 14). As shown in Figure 14, in the recycled catalyst, the dispersion of Pd nanoparticles was almost homogeneous and no aggregation was detected, indicating that recycling did not induce significant morphological change and Pd aggregation.

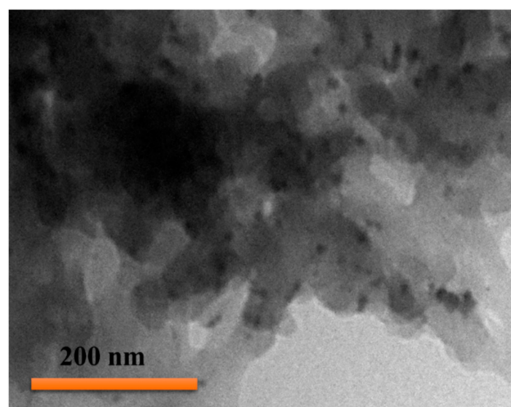


Figure 14. TEM image of the reused catalyst after seven runs.

2.8. Hot Filtration Test

In the final part of this research, a hot filtration test was conducted to appraise the nature of the catalysis. In this context, the model hydrogenation reaction was halted after a short period of time and the reaction yield was estimated. Then, Pd@Per-P was removed from the reaction media and the reaction was continued with no catalyst. The progress of the hydrogenation reaction was monitored to check whether the reaction proceeded in the absence of Pd@Per-P. It was found that after removal of the catalyst, the hydrogenation yield did not increase. This result ruled out the possibility of Pd leaching and re-deposition in the course of the reaction and confirmed the heterogeneous nature of the catalysis.

3. Materials and Methods

3.1. Materials and Instruments

Per used in this research was obtained from Madan Kavan Co. Tehran, Iran. The list of other chemicals and solvents applied for the synthesis of the catalyst and hydrogenation of nitroarenes are as follows: (3-chloropropyl) trimethoxy silane (CPTMS), *N*-isopropylacrylamide (NIPAM), allylamine (AAm), azobisisobutyronitrile (AIBN), triethylamine (Et_3N), palladium (II) acetate, $\text{Pd}(\text{OAc})_2$, sodium borohydride (NaBH_4), nitroarenes, toluene, ethanol (EtOH), methanol (MeOH), and tetrahydrofuran (THF); all were purchased from Sigma-Aldrich (Germany, Taufkirchen) and used without further purification.

Pd@Per-P formation was affirmed by Fourier transform infrared spectroscopy (FTIR), X-ray diffraction (XRD), thermogravimetric analysis (TGA), transmission electron microscopy (TEM), scanning electron microscopy (SEM), energy-dispersive X-ray spectroscopy (EDS), elemental mapping, and Brunauer–Emmett–Teller (BET). The technical data of the used apparatus are as follows:

A BRUKER TENSOR 35 spectrophotometer 65 (Germany, Berlin) with a scan time of 1 s and spectral resolution of 2 cm^{-1} by using a KBr pellet was used to conduct FTIR spectroscopy. The KBr pellets were fabricated using 1 wt.% of the samples. Room temperature powder XRD patterns were recorded using a Rigaku Ultima IV (Japan, Tokyo) with $\text{Cu K}\alpha$ radiation from a sealed tube. TGA was carried out using a Mettler Toledo instrument (model Leicester, Leicester, UK) with a heating rate of $10\text{ }^\circ\text{C}\cdot\text{min}^{-1}$ from 50 to $800\text{ }^\circ\text{C}$ under O_2 atmosphere. TEM images were recorded on a Phillips EM 208S microscope at 100 kV (USA, Beaverton). EDS and elemental mapping analyses were carried out by Tescan Mira II (Czech Republic, Kohoutovice). BET analysis was conducted using a Belsorp Mini II instrument (BEL Japan, Inc., Osaka, Japan). Pd@Per-P was degassed by heating at $150\text{ }^\circ\text{C}$ for 3 h.

3.2. Catalyst Preparation

3.2.1. Synthesis of Poly(NIPAM-co-AAm): P

To synthesize the polymer, NIPAM (1 g) and AAm (1 g) were dissolved in 30 mL EtOH and mixed under an Ar atmosphere. Then, the temperature was increased to $70\text{ }^\circ\text{C}$ and a

solution of AIBN (0.4 g in EtOH (10 mL)) was added in a dropwise manner. After stirring for 24 h, the reaction was stopped, the reaction solvent was evaporated and the polymer was collected.

3.2.2. Chemical Modification of Per: Synthesis of Per-Cl

In order to functionalize Per surface, Per (2 g) was dispersed in dry toluene (40 mL) with the aid of ultrasonic irradiation (160 W for 30 min). Then, CPTMS (2.30 mL) was added to the mixture and the resultant suspension was refluxed for 24 h. Ultimately, the product, Per-Cl, was collected, washed with toluene, and dried in an oven at 50 °C.

3.2.3. Formation of Per-P Nanocomposite

To graft the as-prepared copolymer, P, on Per-Cl, Et₃N (2.43 mL) was dissolved in EtOH (50 mL) and then added to the mixture of P (2 g) and Per-Cl (2 g). Subsequently, the mixture was refluxed under an Ar atmosphere for 24 h. At the end of the reaction, the solvent was evaporated and the solid product was collected, rinsed with distilled water to remove Et₃N⁺ Cl[−] salt and then dried in an oven at 50 °C.

3.2.4. Immobilization of Pd Nanoparticles on Per-P Nanocomposite: Pd@Per-P

In order to prepare Pd@Per-P, Per-P (1 g) was stirred in toluene (20 mL) in a 2-neck round flask under an Ar atmosphere at room temperature for 30 min. Subsequently, a solution of Pd(OAc)₂ (0.02 g) in toluene (15 mL) was added in a dropwise manner to the aforementioned suspension and stirring was continued for 1 h. Then, a solution of NaBH₄ (0.2 N) in MeOH (20 mL) was slowly added to the mixture to reduce Pd(II) to Pd(0). After stirring for 2 h, the as-prepared Pd@Per-P was filtered, washed with toluene, and dried in an oven at 50 °C. The synthetic method for the preparation of Pd@Per-P is illustrated in Figure 1. The ICP analysis of the catalyst established that the content of Pd was 1 wt.%.

3.3. Typical Procedure for Hydrogenation of Nitroarenes

In order to hydrogenize the nitroarenes, a nitro aromatic compound (1 mmol) was dissolved in H₂O/EtOH (1:1) and mixed with the catalyst (30 mg, containing 0.3 mg Pd). Then, the reaction mixture was heated to 45 °C and H₂ gas (1 atm) was purged into the reactor. The progress of the hydrogenation reaction was monitored by TLC and at the end of the reaction, the reaction mixture was cooled down and the catalyst was filtered. The recovered catalyst was washed repeatedly with toluene and dried at 50 °C in an oven. Then, it was used for the second run of the reaction. The aromatic amine was achieved after evaporation of the solvent. The reaction yield was estimated via GC analysis.

4. Conclusions

Cl-functionalized Per was reacted with a thermo-responsive polymer, prepared from co-polymerization of NIPAM and AAm, to give a thermo-responsive composite, Per-P. Then, Pd nanoparticles were stabilized on the as-prepared composite to furnish an efficient catalyst for the hydrogenation of nitroarenes under mild reaction conditions. Study of the reaction temperature indicated that the catalytic activity of the catalyst, Pd@Per-P, was higher at a temperature above LCST. This issue was attributed to the collapse of the polymeric component and formation of a hydrophobic environment that was beneficial for the mass-transfer of the hydrophobic substrates. Using this protocol, various substrates with different steric and electronic properties could be hydrogenated to furnish the corresponding products in high yields. Furthermore, the catalyst was highly selective toward the hydrogenation of nitro functionalities. The recycling test also affirmed high recyclability of the catalyst and low Pd leaching. Regarding the nature of the catalysis, the hot filtration test affirmed that the catalysis was heterogeneous. It was also found that the catalytic activity of the catalyst was higher than that of Pd@Per and Pd@P. This issue was attributed to the possible synergistic effects between two components.

Author Contributions: Conceptualization, S.S. and M.M.H.; Methodology, N.A.-D.; Validation, S.S.; Formal analysis, N.A.-D.; Investigation, resources, S.S. and M.M.H.; Data curation, N.A.-D.; Writing—original draft preparation, S.S.; Writing—review and editing S.S.; Visualization, N.A.-D.; Supervision, S.S. and M.M.H.; Project administration, S.S. and M.M.H.; Funding acquisition, S.S. and M.M.H. All authors have read and agreed to the published version of the manuscript.

Funding: This research received no external funding.

Data Availability Statement: The data presented in this study are available in the article.

Acknowledgments: The authors appreciate the partial support of Iran Polymer and Petrochemical Institute and Alzahra University.

Conflicts of Interest: The authors declare no conflict of interest.

References

- Kolvari, E.; Koukabi, N.; Hosseini, M.M. Perlite: A cheap natural support for immobilization of sulfonic acid as a heterogeneous solid acid catalyst for the heterocyclic multicomponent reaction. *J. Mol. Catal. A Chem.* **2015**, *397*, 68–75. [\[CrossRef\]](#)
- Kolvari, E.; Koukabi, N.; Hosseini, M.M.; Khandani, Z. Perlite: An inexpensive natural support for heterogenization of HBF₄. *RSC Adv.* **2015**, *5*, 36828–36836. [\[CrossRef\]](#)
- Nasrollahzadeh, M.; Sajadi, S.M.; Rostami-Vartooni, A.; Bagherzadeh, M.; Safari, R. Immobilization of copper nanoparticles on perlite: Green synthesis, characterization and catalytic activity on aqueous reduction of 4-nitrophenol. *J. Mol. Catal. A Chem.* **2015**, *400*, 22–30. [\[CrossRef\]](#)
- Kara, G.K.; Rahimi, J.; Niksefat, M.; Taheri-Ledari, R.; Rabbani, M.; Maleki, A. Preparation and characterization of perlite/V₂O₅ nano-spheres via a novel green method: Applied for oxidation of benzyl alcohol derivatives. *Mater. Chem. Phys.* **2020**, *250*, 122991. [\[CrossRef\]](#)
- Akcam, O.; Karaca, E. Development of water vapor resistance feature of polyester woven fabrics by using perlite additive. *J. Text. Appar. Tekst. Konfeksiyon* **2013**, *23*, 233–240.
- Talip, Z.; Eral, M.; Hiçsönmez, Ü. Adsorption of thorium from aqueous solutions by perlite. *J. Environ. Radioact.* **2009**, *100*, 139–143. [\[CrossRef\]](#) [\[PubMed\]](#)
- Yilmazer, S.; Ozdeniz, M.B. The effect of moisture content on sound absorption of expanded perlite plates. *Build. Environ.* **2005**, *40*, 311–318. [\[CrossRef\]](#)
- Bektas, F.; Turanli, L.; Monteiro, P. Use of perlite powder to suppress the alkali-silica reaction. *Cem. Concr. Res.* **2005**, *35*, 2014–2017. [\[CrossRef\]](#)
- Sengul, O.; Azizi, S.; Karaosmanoglu, F.; Tasdemir, M.A. Effect of expanded perlite on the mechanical properties and thermal conductivity of lightweight concrete. *Energy Build.* **2011**, *43*, 671–676. [\[CrossRef\]](#)
- Hosseini, S.; Borghai, S.; Vossoughi, M.; Taghavinia, N. Immobilization of TiO₂ on perlite granules for photocatalytic degradation of phenol. *Appl. Catal. B Environ.* **2007**, *74*, 53–62. [\[CrossRef\]](#)
- Erdem, T.; Meral, Ç.; Tokyay, M.; Erdoğan, T. Use of perlite as a pozzolanic addition in producing blended cements. *Cem. Concr. Compos.* **2007**, *29*, 13–21. [\[CrossRef\]](#)
- Lee, W.; Van Deventer, J. Use of infrared spectroscopy to study geopolymerization of heterogeneous amorphous aluminosilicates. *Langmuir* **2003**, *19*, 8726–8734. [\[CrossRef\]](#)
- Shavisi, Y.; Sharifnia, S.; Hosseini, S.; Khadivi, M. Application of TiO₂/perlite photocatalysis for degradation of ammonia in wastewater. *J. Ind. Eng. Chem.* **2014**, *20*, 278–283. [\[CrossRef\]](#)
- Maryami, M.; Nasrollahzadeh, M.; Sajadi, S.M. Green synthesis of the Pd/perlite nanocomposite using *Euphorbia neriifolia* L. leaf extract and evaluation of its catalytic activity. *Sep. Purif. Technol.* **2017**, *184*, 298–307. [\[CrossRef\]](#)
- Xiao, Y.-Y.; Gong, X.-L.; Kang, Y.; Jiang, Z.-C.; Zhang, S.; Li, B.-J. Light-, pH- and thermal-responsive hydrogels with the triple-shape memory effect. *Chem. Commun.* **2016**, *52*, 10609–10612. [\[CrossRef\]](#)
- Li, J.; Zhou, M.; Ye, Z.; Wang, H.; Ma, C.; Huo, P.; Yan, Y. Enhanced photocatalytic activity of g-C₃N₄-ZnO/HNTs composite heterostructure photocatalysts for degradation of tetracycline under visible light irradiation. *RSC Adv.* **2015**, *5*, 91177–91189. [\[CrossRef\]](#)
- Roy, D.; Brooks, W.L.; Sumerlin, B.S. New directions in thermoresponsive polymers. *Chem. Soc. Rev.* **2013**, *42*, 7214–7243. [\[CrossRef\]](#)
- Jiang, H.; Kelch, S.; Lendlein, A. Polymers move in response to light. *Adv. Mater.* **2006**, *18*, 1471–1475. [\[CrossRef\]](#)
- Ahn, Y.; Jang, Y.; Selvapalam, N.; Yun, G.; Kim, K. Supramolecular velcro for reversible underwater adhesion. *Angew. Chem. Int. Ed.* **2013**, *52*, 3140–3144. [\[CrossRef\]](#)
- Guo, J.; Yuan, C.; Guo, M.; Wang, L.; Yan, F. Flexible and voltage-switchable polymer velcro constructed using host-guest recognition between poly (ionic liquid) strips. *Chem. Sci.* **2014**, *5*, 3261–3266. [\[CrossRef\]](#)
- Chen, F.; Ren, Y.; Guo, J.; Yan, F. Thermo- and electro-dual responsive poly (ionic liquid) electrolyte based smart windows. *Chem. Commun.* **2017**, *53*, 1595–1598. [\[CrossRef\]](#) [\[PubMed\]](#)

22. Moon, H.C.; Lodge, T.P.; Frisbie, C.D. Solution processable, electrochromic ion gels for sub-1 V, flexible displays on plastic. *Chem. Mater.* **2015**, *27*, 1420–1425. [\[CrossRef\]](#)
23. Beaujuge, P.M.; Reynolds, J.R. Color control in π -conjugated organic polymers for use in electrochromic devices. *Chem. Rev.* **2010**, *110*, 268–320. [\[CrossRef\]](#) [\[PubMed\]](#)
24. Massaro, M.; Schembri, V.; Campisciano, V.; Cavallaro, G.; Lazzara, G.; Milioto, S.; Noto, R.; Parisi, F.; Riela, S. Design of PNIPAAm covalently grafted on halloysite nanotubes as a support for metal-based catalysts. *RSC Adv.* **2016**, *6*, 55312–55318. [\[CrossRef\]](#)
25. Shibayama, M.; Suetoh, Y.; Nomura, S. Structure relaxation of hydrophobically aggregated poly (N-isopropylacrylamide) in water. *Macromolecules* **1996**, *29*, 6966–6968. [\[CrossRef\]](#)
26. Gao, C.; Möhwald, H.; Shen, J. Thermosensitive poly (allylamine)-g-poly (N-isopropylacrylamide): Synthesis, phase separation and particle formation. *Polymer* **2005**, *46*, 4088–4097. [\[CrossRef\]](#)
27. Latypova, A.R.; Lebedev, M.D.; Tarasyuk, I.A.; Sidorov, A.I.; Rumyantsev, E.V.; Vashurin, A.S.; Marfin, Y.S. Sol-Gel Synthesis of Organically Modified Silica Particles as Efficient Palladium Catalyst Supports to Perform Hydrogenation Process. *Catalysts* **2021**, *11*, 1175. [\[CrossRef\]](#)
28. Khajonvittayakul, C.; Tongnan, V.; Amornraksa, S.; Laosiripojana, N.; Hartley, M.; Hartley, U.W. CO₂ Hydrogenation to Synthetic Natural Gas over Ni, Fe and Co-Based CeO₂-Cr₂O₃. *Catalysts* **2021**, *11*, 1159. [\[CrossRef\]](#)
29. Metin, Ö.; Can, H.; Şendil, K.; Gültekin, M.S. Monodisperse Ag/Pd core/shell nanoparticles assembled on reduced graphene oxide as highly efficient catalysts for the transfer hydrogenation of nitroarenes. *J. Colloid Interface Sci.* **2017**, *498*, 378–386. [\[CrossRef\]](#) [\[PubMed\]](#)
30. Parida, K.; Varadwaj, G.B.B.; Sahu, S.; Sahoo, P.C. Schiff base Pt (II) complex intercalated montmorillonite: A robust catalyst for hydrogenation of aromatic nitro compounds at room temperature. *Ind. Eng. Chem. Res.* **2011**, *50*, 7849–7856. [\[CrossRef\]](#)
31. Song, J.; Huang, Z.-F.; Pan, L.; Li, K.; Zhang, X.; Wang, L.; Zou, J.-J. Review on selective hydrogenation of nitroarene by catalytic, photocatalytic and electrocatalytic reactions. *Appl. Catal. B* **2018**, *227*, 386–408. [\[CrossRef\]](#)
32. Dehghani, S.; Sadjadi, S.; Bahri-Laleh, N.; Nekoomanesh-Haghighi, M.; Poater, A. Study of the effect of the ligand structure on the catalytic activity of Pd@ ligand decorated halloysite: Combination of experimental and computational studies. *Appl. Organomet. Chem.* **2019**, *33*, e4891. [\[CrossRef\]](#)
33. Sadjadi, S.; Lazzara, G.; Heravi, M.M.; Cavallaro, G. Pd supported on magnetic carbon coated halloysite as hydrogenation catalyst: Study of the contribution of carbon layer and magnetization to the catalytic activity. *Appl. Clay Sci.* **2019**, *182*, 105299. [\[CrossRef\]](#)
34. Sadjadi, S. Halloysite-based hybrids/composites in catalysis. *Appl. Clay Sci.* **2020**, *189*, 105537. [\[CrossRef\]](#)
35. Leonhardt, S.E.S.; Stolle, A.; Ondruschka, B.; Cravotto, G.; Leo, C.D.; Jandt, K.D.; Keller, T.F. Chitosan as a support for heterogeneous Pd catalysts in liquid phase catalysis. *Appl. Catal. A Gen.* **2010**, *379*, 30–37. [\[CrossRef\]](#)
36. Tabrizi, M.; Sadjadi, S.; Pareras, G.; Nekoomanesh-Haghighi, M.; Bahri-Laleh, N.; Poater, A. Efficient hydro-finishing of polyalphaolefin based lubricants under mild reaction condition using Pd on ligands decorated halloysite. *J. Colloid Interface Sci.* **2021**, *581*, 939–953. [\[CrossRef\]](#)
37. Karimi, S.; Bahri-Laleh, N.; Pareras, G.; Sadjadi, S.; Nekoomanesh-Haghighi, M.; Poater, A. Pd on nitrogen rich polymer-halloysite nanocomposite as an environmentally benign and sustainable catalyst for hydrogenation of polyalphaolefin based lubricants. *J. Ind. Eng. Chem.* **2021**, *97*, 441–451. [\[CrossRef\]](#)
38. Saufi, H.; El Alouani, M.; Alehyen, S.; El Achouri, M.; Aride, J. Photocatalytic degradation of methylene blue from aqueous medium onto perlite-based geopolymer. *Int. J. Chem. Eng.* **2020**, *2020*, 9498349. [\[CrossRef\]](#)
39. Zujovic, Z.; Wheelwright, W.V.K.; Kilmartin, P.A.; Hanna, J.V.; Cooney, R.P. Structural investigations of perlite and expanded perlite using ¹H, ²⁷Al and ²⁹Si solid-state NMR. *Ceram. Int.* **2018**, *44*, 2952–2958. [\[CrossRef\]](#)
40. Sadjadi, S.; Heravi, M.M.; Malmir, M.; Masoumi, B. HPA decorated Halloysite Nanoclay: An efficient catalyst for the green synthesis of Spirooxindole derivatives. *Appl. Organomet. Chem.* **2018**, *32*, e4113. [\[CrossRef\]](#)
41. Park, C.-Y.; Lee, Y.-G.; Oh, C.; Oh, S.-G. Preparation of poly-(NIPAM) grafted hybrid silica particles with hollow structure in emulsion. *J. Ind. Eng. Chem.* **2010**, *16*, 32–38. [\[CrossRef\]](#)
42. Sarkar, D.; El Khoury, J.M.; Lopina, S.T.; Hu, J. Grafting poly (t-butyl acrylate) to poly (allylamine) by inverse microemulsion radical polymerization: From comb-polymer to amphiphilic shell crosslinked polymer nanocapsule. *J. Appl. Polym. Sci.* **2007**, *104*, 1905–1911. [\[CrossRef\]](#)
43. Sadjadi, S.; Atai, M. Palladated halloysite hybridized with photo-polymerized hydrogel in the presence of cyclodextrin: An efficient catalytic system benefiting from nanoreactor concept. *Appl. Organomet. Chem.* **2019**, *33*, e4776. [\[CrossRef\]](#)
44. Agrahari, S.; Lande, S.; Balachandran, V.; Kalpana, G.; Jasra, R. Palladium Supported on Mesoporous Alumina Catalyst for Selective Hydrogenation. *J. Nanosci. Curr. Sci.* **2017**, *2*, 2572. [\[CrossRef\]](#)
45. Sadjadi, S.; Koohestani, F.; Bahri-Laleh, N. Pd immobilization on the multi-amine functionalized halloysite as an efficient catalyst for hydrogenation reaction: An experimental and computational study. *Appl. Clay Sci.* **2020**, *192*, 105645. [\[CrossRef\]](#)
46. Samsonu, D.; Brahmaya, M.; Govindh, B.; Murthy, Y. Green synthesis & catalytic study of sucrose stabilized Pd nanoparticles in reduction of nitro compounds to useful amines. *S. Afr. J. Chem. Eng.* **2018**, *25*, 110–115.
47. Esmaeilzadeh, M.; Sadjadi, S.; Salehi, Z. Pd immobilized on hybrid of magnetic graphene quantum dots and cyclodextrin decorated chitosan: An efficient hydrogenation catalyst. *Int. J. Biol. Macromol.* **2020**, *150*, 441–448. [\[CrossRef\]](#) [\[PubMed\]](#)

-
48. Guo, M.; Li, H.; Ren, Y.; Ren, X.; Yang, Q.; Li, C. Improving catalytic hydrogenation performance of Pd nanoparticles by electronic modulation using phosphine ligands. *ACS Catal.* **2018**, *8*, 6476–6485. [[CrossRef](#)]
 49. Sadjadi, S.; Akbari, M.; Leger, B.; Monflier, E.; Heravi, M. Eggplant-derived biochar-halloysite nanocomposite as supports of Pd nanoparticles for the catalytic hydrogenation of nitroarenes in presence of cyclodextrin. *ACS Sustain. Chem. Eng.* **2019**, *7*, 6720–6731. [[CrossRef](#)]
 50. Sadjadi, S.; Ghoreyshi Kahangi, F.; Heravi, M.M. Pd stabilized on nanocomposite of halloysite and β -cyclodextrin derived carbon: An efficient catalyst for hydrogenation of nitroarene. *Polyhedron* **2020**, *175*, 114210. [[CrossRef](#)]